System mass optimization of hydrogen/oxygen based regenerative fuel cells for geosynchronous space missions

S. Hauff and K. Bolwin*

German Aerospace Research Establishment (DLR), Institute for Technical Thermodynamics, Pfaffenwaldring 38-40, 7000 Stuttgart 80 (FRG)

(Received August 10, 1991; in revised form November 7, 1991)

Abstract

A major disadvantage of conventional battery systems is the strong coupling between their capacity and rated power determined by the energy storage per unit area of the electrodes. For regenerative fuel cell systems these parameters are decoupled, since their capacity is directly related to the fuel storage, while the rated power depends on the electrode area. This intrinsic advantage of the RFC system permits design optimization by varying the current density of both elements, the electrolyzer and the fuel cell stack, and evaluating the masses of the two subsystems. Mass optimization has been carried out considering a dedicated electrolyzer and fuel cell system, together with the masses of a photovoltaic array, a radiator and the required storage. The energy storage capacity has been designed for the limiting conditions of a geosynchronous earth orbit (GEO) mission and a mean power requirement of 25 kW.

1. Introduction

The use of fuel cells with related electrolyzers may be a favoured approach both to reduce the cost of orbit insertion as well as fuel replacement for energy supply systems for future long-term space missions. Recently it was shown that regenerative fuel cell (RFC) systems for space applications may have distinct design advantages compared with state-of-the-art battery systems [1–3]. An additional advantage arises from their ability to integrate with the propulsion fuel supply.

The present work is a summary of our recent investigations into the potential for system mass reduction through optimization of the operating conditions of associated fuel cells and electrolyzers. This optimization was performed by varying the current densities of both the fuel cell and the electrolyzer. Efficiency and waste heat production have been calculated assuming characteristics of different state-of-the-art cell stacks in alkaline and proton exchange membrane (PEM) technology. Since the optimized operating point is strongly influenced by the selected characteristics of the electrochemical components, additional calculations were performed assuming future cell performance parameters.

Finally, comparisons with both conventional energy storage systems (e.g. Ni/H_2 batteries or latent heat storage) and regenerative energy storage, based on alternative

*Author to whom correspondence should be addressed.

0378-7753/92/$5.00

electrochemical reactions (e.g. the carbon monoxide fuel cell reaction $2CO + O_2 \rightarrow 2CO_2$) are given.

2. Results and discussion

2.1. Description of the RFC system

Optimization of the system mass was performed by considering an RFC system consisting of dedicated electrochemical cell stacks (fuel cell and electrolyzer), fuel storage, a photovoltaic array as the primary energy supply, and a radiator to reject the waste heat. A schematic energy storage concept system is shown in Fig. 1.

The capacities of these components of the RFC are correlated by various relations to each other. The design of the RFC system is determined by the limiting conditions of the space mission (e.g. rated power, orbit altitude) and the characteristics of the electrochemical cells. Performing the optimization of the entire system mass, the capacities of the system components have to be expressed in terms of these fundamental values. As a first estimate, the power output of the electrochemical stack is related to the electrode area and the number of cells within the stack by eqns. (1) and (2):

$$A_{fc} n_{fc} = \frac{P_r}{i_{fc} u_{fc}(i_{fc})} \tag{1}$$

$$A_{el} n_{el} = \frac{P_r}{i_{el} u_{el}(i_{el}) \eta_{fc}(i_{fc})} \frac{t_e}{t_s} \tag{2}$$

for the fuel cell and the electrolyzer, respectively, where i_c and u_c denote the current density and cell voltage of the considered cells; P_r denotes the rated power; t_e and t_s denote the period of the eclipse and sunshine phase, respectively. The efficiency of the fuel cell $\eta_{fc} = u_{fc}/u_0$ is related to the thermoneutral voltage $u_0 = zF/\Delta H$, where F is Faradays constant and ΔH and z denote the reaction enthalpy and the valence of the ions, respectively, that are responsible for the charge transfer in this reaction. The power output of the electrolyzer P_{el} in terms of enthalpy differences coupled with the mass flow of H_2 and O_2, is determined by the efficiency of the fuel cell η_{fc} and the limiting conditions of the geosynchronous orbit: $t_e/t_s = \arcsin(R/r)/(\pi - \arcsin(R/r)) = 0.0508$ (r and R denote the radii of the earth and the geosynchronous orbit, respectively).

$$P_{el} = 0.0508 P_r \frac{1}{\eta_{fc}} \tag{3}$$

Evaluating the system mass of the electrochemical components, it is obvious that the mass of the cell stack itself is related to the entire electrode surface $A_{el} n_{el}$; however, additional peripheral components contribute to the entire system mass. These contributions are directly related to the power of the electrochemical cells ($P_{out} = P_r$, P_{el} for the fuel cell and electrolyzer, respectively). This leads to a slightly more complex relation for the subsystem mass of both the fuel cell and the electrolyzer:

$$m_C = \rho_{C,ST} A_C n_C + \rho_{C,P} P_{C,out} \tag{4}$$

where ρ denote the specific masses of both the cell stack and the periphery, as indicated by the indices ST and P, respectively.

Recently calculations of fuel storage masses have been given depending on the required storage capacity [2, 4]. These relationships could be approximated sufficiently

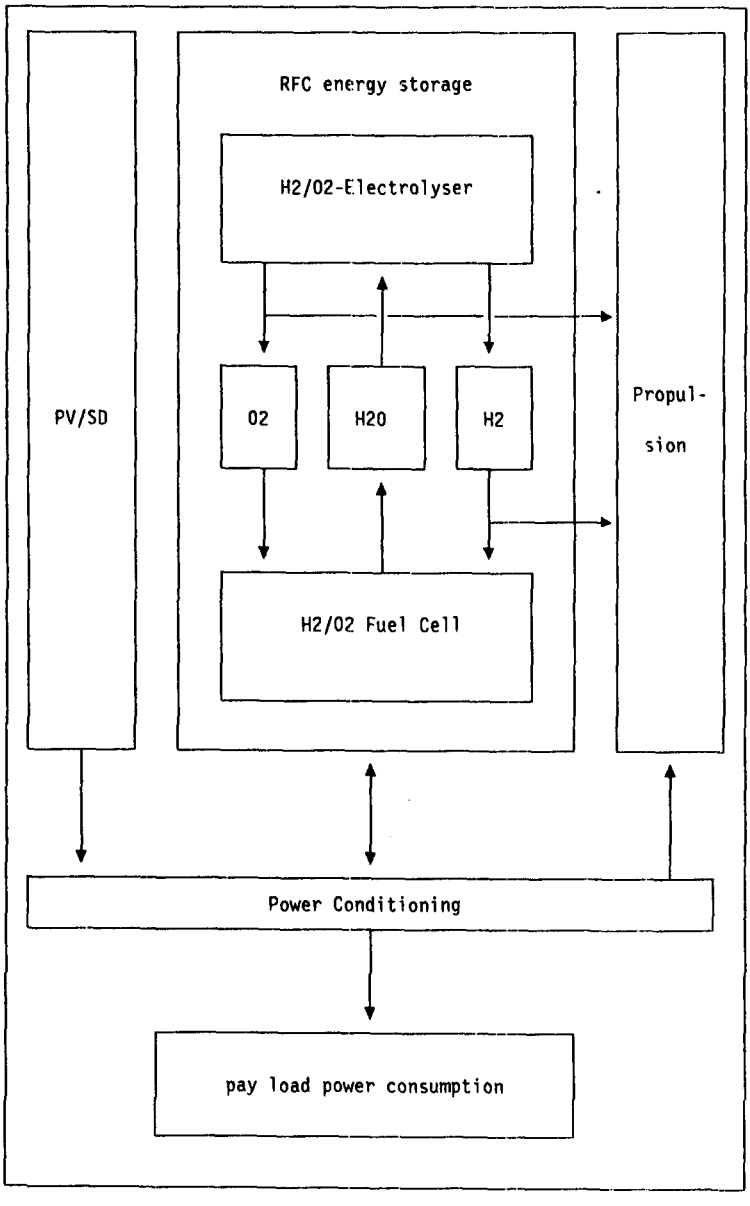

Fig. 1. Draft of the regenerative fuel cell.

by linear expressions, as given in eqn. (5):

$$m_{H_2,ST} = 50 + 18.75 m_{H_2}$$
$$m_{O_2,ST} = 50 + 0.15 m_{O_2} \quad (5)$$
$$m_{H_2O,ST} = 5 + 0.075 m_{H_2O}$$

where $m_{x,ST}$ and m_x ($x = H_2, O_2, H_2O$) denote the masses of the stores and the masses of the stored fuels, respectively.

Finally, the amount of fuel, that has to be stored, depends on the required energy E_{st}, that is needed to secure the power supply during the eclipse phase:

$$m_x = \frac{E_{st}}{\Delta H_{Reaction}} \tag{6}$$

where ΔH denotes the enthalpy variation of the hydrogen/oxygen reaction in (kJ/kg) (see Table 1), and the required energy is given by eqn. (7):

$$E_{st} = P_r \frac{1}{\eta_{fc}} t_e \tag{7}$$

From eqns. (5) and (6), we deduce the following relation, that describes the entire storage mass as a function of fundamental system parameters:

$$m_{st} = 50 + 1.3111 \times 10^{-4} E_{st} + 50 + 0.0839 \times 10^{-4} E_{st} + 5 + 0.0472 \times 10^{-4} E_{st}$$
$$= 105 + 1.4422 \times 10^{-4} E_{st} \tag{8}$$

Assuming a steady energy consumption of P_r, during the entire orbit period, the required primary power to operate the electrolyzer can be expressed by:

$$P_{pr} = 0.0508 \times P_r \frac{1}{\eta_{fc}\eta_{el}} \tag{9}$$

and the mass of the photovoltaic array can be expressed by:

$$m_{PV} = \rho_{PV} P_{pr} \tag{10}$$

Finally the capacity of the radiator is related to the waste heat production rate. Since the efficiency of the fuel cell is due to the entropy variation lower than that of the electrolyzer, waste heat production occurs mainly during the eclipse phase. On the other hand it may be advantageous to store thermal energy, if the electrolyzer could be operated below the thermoneutral voltage u_0 or waste heat should be used to keep the temperature level during non-operation of the stack. Thus, the capacity of the radiator is related to the waste heat production rate of the fuel cell ($\dot{Q}_{fc}$), reduced by the amount of thermal energy, that could be recycled into the process. The waste heat production rate is determined from the efficiency of the fuel cell:

$$\dot{Q}_{fc} = P_r \left(\frac{1}{\eta_{fc}} - 1 \right) \tag{11}$$

Using Q and Q' as the amounts of waste heat which are utilizable or that have to be stored, then the masses of the radiator and thermal storage can be expressed by eqns. (12) and (13), respectively:

$$m_{rad} = \rho_{rad} \left(\dot{Q}_{fc} - \frac{Q}{t_e} \right) \tag{12}$$

$$m_{th,st} = \left(1 + \frac{m_{cont}}{m_m} \right) \frac{Q'}{\Delta H_{melt}} \tag{13}$$

Equation (13) has been deduced, assuming a latent heat storage based on $AlCl_3$–KCl–LiCl as the storage medium, m_{cont} and m_m denote the masses of the

containment and the storage medium respectively, the ratio of these masses is assumed to be $m_{cont}/m_m = 0.3$. The melting enthalpy ΔH_{melt} is given in Table 1. For a detailed description of the thermal flows, see Fig. 2. The utilizable waste heat Q can expressed as:

$$Q = Q' + \dot{Q}_{el} t_e \tag{14a}$$

with

$$Q' = (\dot{Q}_{fc,s} - \dot{Q}_{el,s}) \frac{t_s}{\eta_{st}} = \left(\dot{Q}_{fc,s} - \left(1 - \frac{u_0}{u_{el}(i_{el})} \right) P_{el} \right) \frac{t_s}{\eta_{st}} \tag{14b}$$

where Q' denotes the thermal energy, that has been stored during the eclipse phase and the storage efficiency is assumed to be $\eta_{st} = 0.9$.

From eqns. (1)–(13), it is found that the masses of the system components are influenced mainly by the efficiency of both the electrolyzer and the fuel cell. From this, mass optimization has been performed on the basis of different characteristics, considering alkaline and PEM technology. Figure 3 shows the characteristics of both state-of-the-art and advanced cell technology as used in the calculations. However the result does not only depend on the assumed cell characteristics, but also on the specific weights of the RFC subsystems. The values used in the present optimization are given in Table 1. Improving the designs of the subsystems, these data may vary and affect the result of the optimization.

From the flat slope of the advanced cell characteristics, we suppose a decreasing dependency of the optimized operating point on the entire efficiency. This means that the stack weight of the electrochemical components receives increasing importance for the system mass optimization.

TABLE 1

Characteristic values of the subsystems as used in the calculation

Symbol	Value	Unit	Description
ρ_{ST}	18.645[a]	kg/m^2	specific mass of the electrochemical cell stack
ρ_P	6.451[a]	kg/kW	specific mass of peripheral components of the electrochemical cells
ρ_{rad}	24.26[b]	kg/kW	specific mass of the radiator
ρ_{PV}	18.0[b]	kg/kW	specific mass of the photovoltaic array
ΔH_{melt}	195	kJ/kg	melting enthalpy of the latent heat storage under consideration
m_{react}	6.3×10^{-5}	kg/kJ	specific reactant consumption during eclipse period
$\Delta H_{reaction}$	1.43×10^5 1.78×10^4 1.59×10^4	kJ/kg$_{H_2}$ kJ/kg$_{O_2}$ kJ/kg$_{H_2O}$	enthalpy variation of the hydrogen/oxygen reaction

[a]From ref. 5.
[b]From ref. 2.

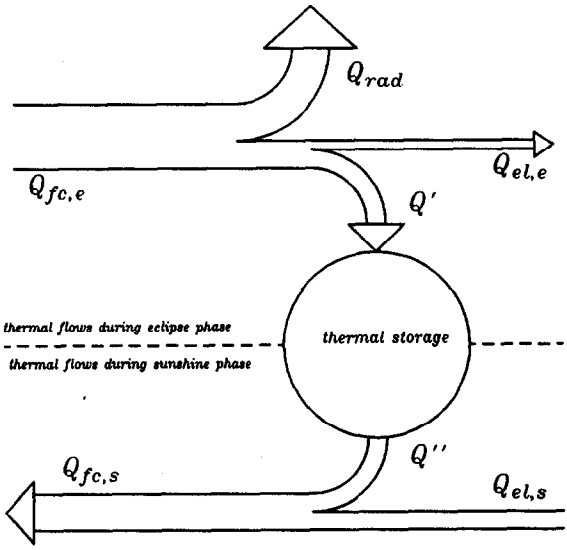

Fig. 2. Draft of thermal flows in the RFC system. The waste heat is used for temperature keeping during disoperation of an electrochemical cell. $\dot{Q}_{fc,e}$, $\dot{Q}_{el,e}$, $\dot{Q}_{fc,s}$ and $\dot{Q}_{el,s}$ denote the thermal flows across the surfaces of the fuel cell and electrolyzer during eclipse and sunshine phase, respectively.

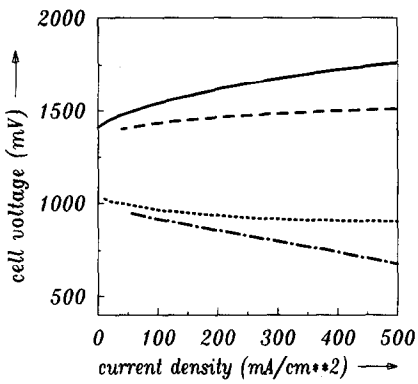

Fig. 3. Characteristics of different electrochemical cells. Solid line: Hydrogen Systems alkaline electrolyzer (T=353 K, p=2 bar); dashed line: ABB PEM electrolyzer (T=373 K, p=2 bar); dotted line: UTC PEM fuel cell (T=394 K, p=4.14 bar); dash-dotted line: Siemens alkaline fuel cell (T=353 K, p=2 bar).

2.2. *System mass optimization*

Minimization of the stack weight of both fuel cell and electrolyzer leads to a cell operation with high current densities; however maximization of the storage efficiency results in operating these components with low current densities. Since the system mass depends on the storage efficiency (see eqns. (1)–(12)) and, on the other hand, the stack weight contributes directly to this value, the determination of the operating

point is an optimization problem regarding the current densities of fuel cell and electrolyzer.

The result of an optimization, based on approved cell characteristics, is shown in Fig. 4. The current densities have been varied between 50 and 475 mA/cm^2 for both fuel cell and electrolyzer. Parameter variation above $i = 475$ mA/cm^2 could not be performed, since data of cell characteristics were not available for high current density operation. The data are presented in both a 3D-diagram and a level chart. In the level chart the solid and the dashed lines are spaced by 50 kg and 10 kg, respectively.

Evaluating the system mass, a distinct minimum is found at a current density of $i_{fc} = 240$ mA/cm^2 for fuel cell operation. However the current density of the electrolyzer can vary over a wide range ($i_{el} > 150$ mA/cm^2) without significant changes in the system mass. The supposed minimum is clearly located beyond $i_{el} = 475$ mA/cm^2. The entire system mass strongly increases, when the current density of the fuel cell either keeps within the range $i_{fc} < 150$ mA/cm^2 or exceeds the limit of $i_{fc} = 350$ mA/cm^2. Additionally, the system mass slightly increases for current densities of the electrolyzer below $i_{el} <$ 150 mA/cm^2. The slight dependency of the system mass on the operation point of the electrolyzer results from the ratio of the operating periods of the fuel cell electrolyzer. Since $t_e/t_s = 0.0508$ (see eqn. (3)), a low power electrolyzer is required only, to ensure the power supply of the eclipse phase.

The stronger increasing system mass for $i_{fc} < 150$ mA/cm^2 is explained by the singularity observed in the electrode area, when the current density becomes zero (see eqn. (1)).

Operating the fuel cell in a high current density mode, the performance losses due to the decreasing efficiency overpower the weight advantages of a smaller, more compact cell stack design.

This behaviour is of general validity; however, mass optimization on the basis of advanced cell characteristics results in a shift of the optimized operating point toward higher current densities of the fuel cell. The supposed minimum of the system mass is located clearly beyond the considered range of fuel cell operation (see Fig. 5). This result is reasonable, since the performance losses become less important, as indicated by the flat slope of the advanced fuel cell characteristics.

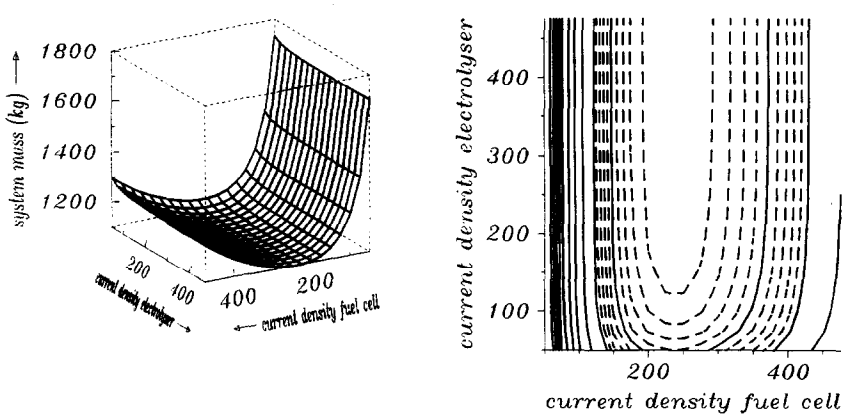

Fig. 4. System mass of a dedicated RFC system for GEO missions. The calculation is based on state-of-the-art cell characteristics (Siemens fuel cell and Hydrogen Systems electrolyzer).

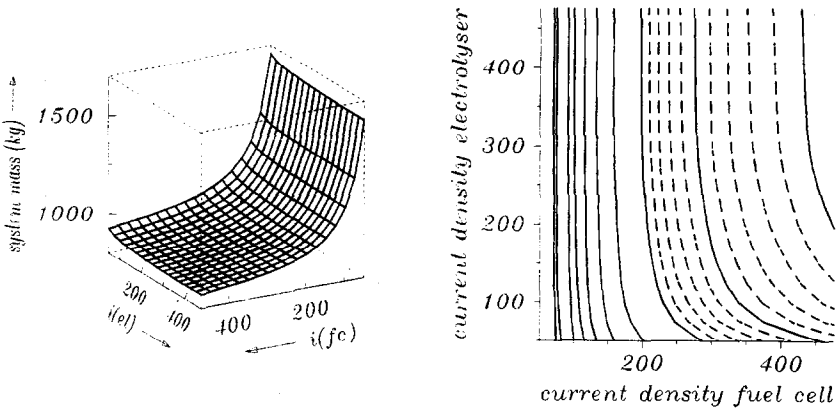

Fig. 5. System mass of a dedicated RFC system for GEO missions. The calculation is based on advanced cell characteristics (UTC fuel cell and ABB SPE electrolyzer).

From this, we deduce a high potential for the system mass reduction due to the development of advanced cell technology and new materials operated as electrocatalysts on the electrode surfaces. Since the system mass again shows only a slight dependence on the electrolyzer operating point, new electrocatalysts for fuel cell operation are especially important.

The mass reduction potential is estimated by a comparison of the data shown in Figs. 4 and 5 for the approved and advanced cell technology, respectively. It is shown that the system mass could be reduced by more than 20% due to advanced electrochemical techniques and optimizing the operating point. Simultaneously, the operating point for the fuel cell is shifted from $i_{fc}=240$ to $i_{fc}\geqslant 475$ mA/cm^2.

Recently we have shown, that the system mass could be reduced by nearly 10% in low earth orbit (LEO) space missions, due to the integration of a larger thermal store and steady waste heat rejection over the entire orbit period [6]. However the integration of thermal storage is disadvantageous for GEO missions. This result is reasonable, since the weight of the thermal storage depends on the waste heat that has to be stored during the eclipse period, whereas the size of the radiator depends only on the rated power of the fuel cell. Since the period of the eclipse phase increases with increasing orbit altitudes higher than 1400 km, the advantage of a steady waste heat rejection becomes less important due to the increasing thermal storage. For the parameter set used in the presented calculation, the concept of an integrated thermal storage is limited to orbits lower than 20 000 km. In the geosynchronous orbit (35 795 km), a thermal storage would increase the system mass by approximately 10%.

Compared to calculations based on the limiting conditions of low earth orbits [6] the operating point of the fuel cell in GEO orbit is shifted to slightly higher current densities (from $i_{fc}=200$ to 240 mA/cm^2), assuming approved cell technologies (see Fig. 6). Here the contours are spaced by 1% of the minimized system mass for both LEO and GEO modelling. The LEO data are indicated by the dashed lines. Note, that the contours represent the system mass with respect to the minimum of each data set; no absolute values are given. From these data, the performance losses of a RFC system due to a deoptimized operating point is estimated to 10%, assuming approved cell technique. Whereas the operating point of the electrolyzer can vary within a wide range in GEO missions, electrolyzer operation is optimized at $i_{el}=375$ mA/cm^2 in low earth orbits. This behaviour is obvious, since in GEO missions

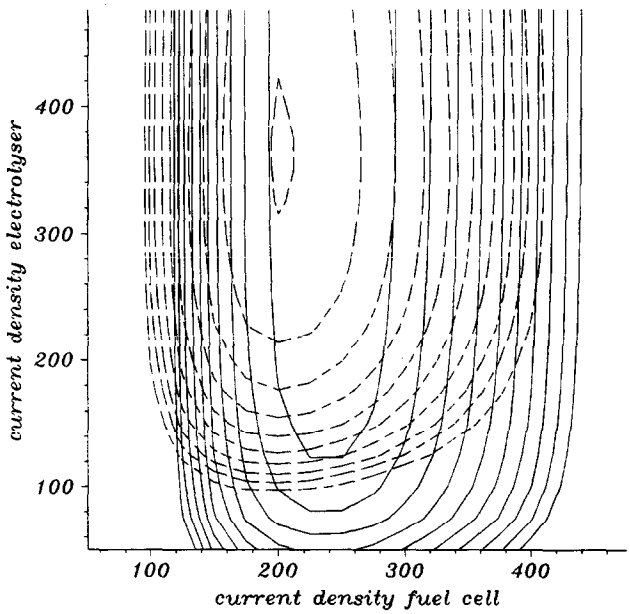

Fig. 6. Comparison of LEO and GEO design points in approved technology.

a low power electrolyzer is required only, to ensure the energy supply during eclipse phase.

2.3. Comparison to battery systems

A major advantage of regenerative energy storage is the possibility to reduce the expense of fuel replacement for space missions by recirculation of the fuel and oxidant flows. In addition, replacement could be performed as water subsequently electrolyzed in space. However the RFC system is more complex than approved, non-regenerative energy storage, e.g. Ni/H_2 batteries. Thus is it necessary to compare the system masses of regenerative energy storage to that of approved technologies.

Recently several regenerative storage concepts have been compared to the system mass of the Ni/H_2 battery [4]. This comparison has been performed assuming a GEO mission and a rated power of 90 kW. Ambient temperatures have been assumed to be 6 and 225 K in the eclipse and sunshine phase, respectively.

The RFC systems under consideration could be classified into three major sections, regarding different type of fuel cell reactions (see Table 2). Both the H_2/O_2- and the CO-RFC are dedicated systems consisting of a fuel cell and an electrolyzer, serving the reverse reaction to 'charge' the RFC. The fuel processing in the CH_4-RFC is more complex, since here the 'charge' reaction forms two branches: water decomposition is carried out in an electrolyzer, whereas the CO_2 is reduced in a Sabatier reactor using hydrogen ($CO_2+4H_2 \rightarrow CH_4+2H_2O$).

The system mass of the Ni/H_2 battery was calculated assuming an energy density of 45 W h/kg and a depth-of-discharge (DOD) of 60%. The storage efficiency was assumed to be η (W h) = 75%.

A brief description of the energy storage systems considered is given in Table 2.

TABLE 2

Brief description of energy storage concepts

No.	Description
1	Ni/H_2 battery (45 W h/kg; 60% DOD)
2	LiF latent heat storage
	H_2/O_2-FC reaction: $2H_2+O_2 \rightarrow 2H_2O+\Delta H$
3	H_2/O_2 low temperature RFC gaseous storage H_2O electrolyzer
4	H_2/O_2 low temperature RFC cryogenic storage H_2O electrolyzer
5	H_2/O_2 high temperature RFC gaseous storage H_2O electrolyzer
6	H_2/O_2 high temperature RFC cryogenic storage H_2O electrolyzer
	Carbon monoxide-FC reaction: $2CO+O_2 \rightarrow 2CO_2+\Delta H$
7	CO high temperature RFC gaseous storage CO_2 electrolyzer
8	CO high temperature RFC cryogenic storage CO_2 electrolyzer
	CH_4-FC reaction: $CH_4+2O_2 \rightarrow 2CO_2+2H_2O+\Delta H$
9	CH_4 high temperature RFC gaseous storage H_2O electrolyzer and Sabatier reactor
10	CH_4 high temperature RFC cryogenic storage H_2O electrolyzer and Sabatier reactor

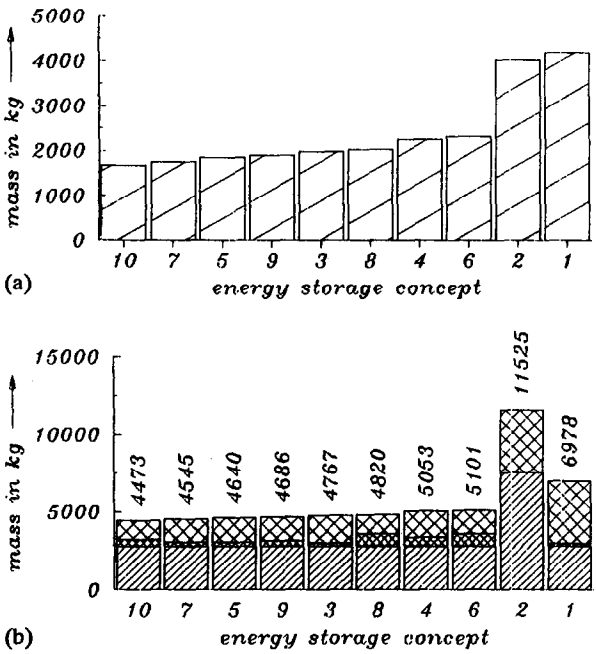

Fig. 7 Comparison of several storage concepts: (a) system mass of the storage concept only; (b) system mass including the primary energy supply.

The first diagram in Fig. 7 gives a comparison of the pure energy storages including all subsystems, e.g. pumps, refrigerators, fuel storages and the primary energy supplier for the eclipse phase. These calculations are based on very advanced data, regarding the specific characteristics of the radiator and electrochemical subsystems [4]:

- efficiency of the electrolyzer: $\eta_{el}=0.96$
- efficiency of the fuel cell: $\eta_{fc}=0.67$
- specific mass of the PV array: $\rho_{PV}=30.9$ kg/kW
- specific mass of the radiator: $\rho_{rad}=6.6$ kg/kW

The next data are valid for the H_2/O_2-RFC systems only:

- specific mass of the electrolyzer: $\rho_{el}=3.2$ kg/kW (SOFC technique)
- specific mass of the fuel cell: $\rho_{fc}=12$ kg/kW

All RFC systems considered show distinct advantages regarding their system mass compared to conventional energy storage. The mass reduction potential of the RFC concepts is estimated to be 50–60% with respect to the Ni/H_2 battery or the latent heat storage, considering the energy storage only. Considering the primary energy supplier, the masses of the regenerative storage concepts have been estimated within the range of 65%–73% of the Ni/H_2 battery. The concept of latent heat storage is not competitive for geosynchronous space missions, since it demands a solar dynamic primary energy supply (see Fig. 7(b)). The masses of the RFC systems range between 38–50% of that of latent heat storage. Whereas cryogenic fuel storage is disadvantageous in the low earth orbit [6], these concepts are competitive in GEO missions. Beyond this, the RFC concept showing the best performance is based on cryogenic storage of methane (see Fig. 7(a) and Table 2). However the other concepts assuming cryogenic storage show slight higher system masses.

However, comparing the system weights of the regenerative energy storage concepts to the mass of Ni/H_2 battery, the result depends on the performance of the battery storage. Improving the design of the Ni/H_2 battery, the advantage of the RFC systems regarding their system weight decreases or vanishes. Nevertheless, the mean system weight of the most favourable regenerative storage concepts is at least 7.5% less than the mass of the Ni/H_2 battery. In Fig. 8 the system mass is shown versus the energy density of the battery; the different curves refer to different depths-of-discharge (DOD) as indicated in the Figure. Although the number of charge/discharge cycles is limited due to a high depth-of-discharge, the battery can be operated over a sufficient period,

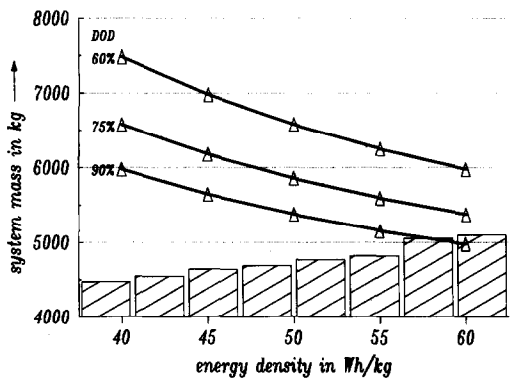

Fig. 8. System mass of a nickel/hydrogen battery storage vs. energy density. Note, that the mass for the primary energy supplier for the entire orbit period is considered in the calculation. The masses of the regenerative storage systems are indicated by the histogram, the bars refer to the storage concepts 3–10, as indicated in Fig. 7, however their position is not related to the energy density scale.

since the number of charge/discharge cycles is limited to 90 cycles per year for the geosynchronous orbit.

However, since the propulsion purposes for orbit control are not integrable into both the conventional battery system and the latent heat storage concept, the regenerative concepts should receive additional advantage, if the integration of these tasks is desired.

3. Conclusions

Advanced performance of the electrocatalytic properties results in increasing current densities for the system design. Regarding the optimization of the system mass, the development of advanced electrodes showing low inclined characteristics for fuel cell and electrolyzer operation is essential. Due to these advanced electrodes the system mass of RFC systems can be reduced for the geosynchronous orbit by more than 20% regarding the optimized operating point in approved cell technique.

The integration of thermal storage to reduce radiator requirements due to steady waste heat rejection is disadvantageous in GEO missions.

Compared to calculations based on the limiting conditions of low earth orbits [6] the operating point of the fuel cell is shifted to slightly higher current densities, assuming approved cell technologies. The design of the electrolyzer is less important in GEO missions, since here the eclipse period is short regarding the entire orbit period, and a highly efficient electrolyzer is not required. A reduction potential of the system mass arises mainly from development of advanced fuel cell technologies.

Finally, comparison of the H_2/O_2-RFC to both other regenerative energy storage concepts and conventional battery systems has shown that the regenerative low temperature H_2/O_2 fuel cell is a competitive concept for future energy supply systems in GEO space missions. Whereas cryogenic fuel storage is disadvantageous in low earth orbit, these concepts are competitive for geosynchronous missions.

List of symbols

A_{fc}	electrode area of a single fuel cell, cm^2
A_{el}	electrode area of a single electrolyzer cell, cm^2
E_{st}	capacity of the electrical storage, kJ
F	Faradays constant, C/mol
i_{fc}	current density of the fuel cell, mA/cm^2
i_{el}	current density of the electrolyzer, mA/cm^2
m_C	mass of the electrochemical cell stack, kg
m_{st}	mass of the fuel storage, kg
m_{PV}	mass of the PV array, kg
m_{rad}	mass of the radiator, kg
$m_{th,st}$	mass of the thermal storage, kg
m_x	mass of the reactants x, kg
n_{fc}	number of cells within the fuel cell stack
n_{el}	number of cells within the electrolyzer stack
P_{el}	output power of the electrolyzer, kW
P_r	output power of the fuel cell, kW
P_{pr}	output power of the polyvoltaic array, kW
Q_{fc}	waste heat of the fuel cell, kW

Q	utilizable waste heat, kW
Q'	capacity of the thermal storage, kW
R	radius of the earth (6378 km), km
r	radius of the geosynchronous orbit (42 173 km), km
t_e	period of the eclipse phase, s
t_s	period of the sunshine phase, s
u_{fc}	voltage at a single fuel cell, V
u_{el}	voltage at a single electrolyzer cell, V
u_0	thermoneutral voltage, V
z	valence of the ions
η_{fc}	efficiency of the fuel cell
η_{el}	efficiency of the electrolyzer
η_{st}	efficiency of the thermal storage
$\Delta H_{reaction}$	enthalpy of the hydrogen/oxygen reaction, kJ/kg
ΔH_{melt}	melting enthalpy of the latent heat storage, kJ/kg
$\rho_{C,ST}$	specific mass of the cell stacks, kg/cm^2
$\rho_{C,P}$	specific mass of the stack periphery, kg/kW
ρ_{PV}	specific mass of the PV array, kg/kW
ρ_{rad}	specific mass of the radiator, kg/kW

References

1 Boeing Aerospace Co., Analysis of regenerative fuel cells, NASA contract NAS9-16151, 1982.
2 DLR, Solar dynamic energy supply systems, BMFT contract 8603/8, 1987.
3 A. Levy, L. L. Van Dine and J. K. Stedman, *NASA Rep. No. NASA CR-179609*, 1987.
4 Dornier GmbH and DLR, Regenerative fuel management in space missions, DARA contract in preparation.
5 *BMFT Research Rep.*, BMFT contract T83-113, 1983.
6 K. Bolwin and S. Hauff, Reduction potential of the system mass of hydrogen/oxygen based regenerative fuel cell systems for LEO application, *Proc. 26th IECEC, Boston, MA, 1991*, Vol. 3, pp. 504–509.